AREVA

March 22, 2012
NRC:12:015

Document Control Desk
U.S. Nuclear Regulatory Commission
Washington, D.C. 20555-0001

Response to U.S. EPR Design Certification Application RAI No. 422, Supplement 35

Ref. 1: E-mail, Getachew Tesfaye (NRC) to Martin C. Bryan (AREVA NP Inc.), "U.S. EPR Design Certification Application RAI No. 422 (4792), FSAR Ch. 3," August 3, 2010.

Ref. 2: E-mail, Dennis Williford (AREVA NP Inc.) to Getachew Tesfaye (NRC), "Response to U.S. EPR Design Certification Application RAI No. 422, FSAR Ch. 3, Supplement 34," February 17, 2012.

In Reference 1, the NRC provided a request for additional information (RAI) regarding the U.S. EPR design certification application. Reference 2 provided a revised schedule for the remaining question (03.09.02-108) and a history of the prior supplemental responses.

Enclosed is a technically correct and complete final response to the remaining question of RAI 422, as shown in the below table.

AREVA NP considers some of the material contained in the attached response to be proprietary. As required by 10 CFR 2.390(b), an affidavit is attached to support the withholding of the information from public disclosure. Proprietary and non-proprietary versions of the enclosure to this letter are provided.

Appended to this file are affected pages of ANP-10306P, "Comprehensive Vibration Assessment Program for U.S. EPR Reactor Internals Technical Report," in redline-strikeout format which support the response to RAI 422 Question 03.09.02-108.

The following table indicates the respective pages in the enclosed response that contain AREVA NP's final response to the subject questions.

Question #	Start Page	End Page
RAI 422 — 03.09.02-108	2	26

D077
NRO

AREVA INC.
3315 Old Forest Road, P.O. Box 10935, Lynchburg, VA 24506-0935
Tel.: 434 832 3000 www.areva.com

This concludes the formal AREVA NP response to RAI 422, and there are no questions from this RAI for which AREVA NP has not provided responses.

If you have any questions related to this submittal, please contact Darrell Gardner by telephone at 704-805-2355 or by e-mail to Darrell.Gardner@areva.com.

Sincerely,

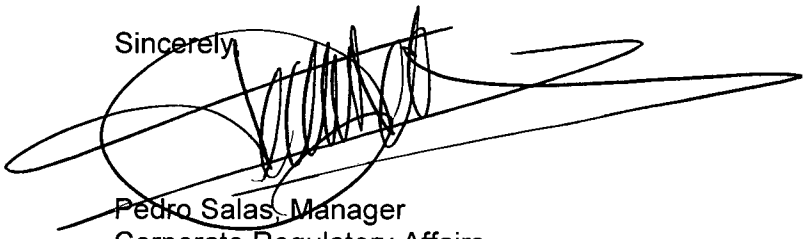

Pedro Salas, Manager
Corporate Regulatory Affairs
AREVA NP Inc.

Enclosures

cc: G. Tesfaye
Docket No. 52-020

AFFIDAVIT

COMMONWEALTH OF VIRGINIA)
) ss.
COUNTY OF CAMPBELL)

1. My name is David K. White. I am Manager, Product Licensing, for AREVA NP Inc. (AREVA NP) and as such I am authorized to execute this Affidavit.

2. I am familiar with the criteria applied by AREVA NP to determine whether certain AREVA NP information is proprietary. I am familiar with the policies established by AREVA NP to ensure the proper application of these criteria.

3. I am familiar with the AREVA NP information contained in the "Response to U.S. EPR Design Certification Application RAI No. 422, Supplement 35," and referred to herein as "Document." Information contained in this Document has been classified by AREVA NP as proprietary in accordance with the policies established by AREVA NP for the control and protection of proprietary and confidential information.

4. This Document contains information of a proprietary and confidential nature and is of the type customarily held in confidence by AREVA NP and not made available to the public. Based on my experience, I am aware that other companies regard information of the kind contained in this Document as proprietary and confidential.

5. This Document has been made available to the U.S. Nuclear Regulatory Commission in confidence with the request that the information contained in this Document be withheld from public disclosure. The request for withholding of proprietary information is made in accordance with 10 CFR 2.390. The information for which withholding from disclosure is

requested qualifies under 10 CFR 2.390(a)(4) "Trade secrets and commercial or financial information".

6. The following criteria are customarily applied by AREVA NP to determine whether information should be classified as proprietary:

(a) The information reveals details of AREVA NP's research and development plans and programs or their results.

(b) Use of the information by a competitor would permit the competitor to significantly reduce its expenditures, in time or resources, to design, produce, or market a similar product or service.

(c) The information includes test data or analytical techniques concerning a process, methodology, or component, the application of which results in a competitive advantage for AREVA NP.

(d) The information reveals certain distinguishing aspects of a process, methodology, or component, the exclusive use of which provides a competitive advantage for AREVA NP in product optimization or marketability.

(e) The information is vital to a competitive advantage held by AREVA NP, would be helpful to competitors to AREVA NP, and would likely cause substantial harm to the competitive position of AREVA NP.

The information in the Document is considered proprietary for the reasons set forth in paragraphs 6(c) and (d) above.

7. In accordance with AREVA NP's policies governing the protection and control of information, proprietary information contained in this Document has been made available, on a limited basis, to others outside AREVA NP only as required and under suitable agreement providing for nondisclosure and limited use of the information.

8. AREVA NP policy requires that proprietary information be kept in a secured file or area and distributed on a need-to-know basis.

9. The foregoing statements are true and correct to the best of my knowledge, information, and belief.

David K. White

SUBSCRIBED before me this 22nd day of March, 2012.

Kathleen A. Bennett

Kathleen A. Bennett
NOTARY PUBLIC, COMMONWEALTH OF VIRGINIA
MY COMMISSION EXPIRES: 8/31/2015
Reg. #110864

KATHLEEN ANN BENNETT
Notary Public
Commonwealth of Virginia
110864
My Commission Expires Aug 31, 2015

Response to

Request for Additional Information No. 422, Supplement 35

8/3/2010

U. S. EPR Standard Design Certification
AREVA NP Inc.
Docket No. 52-020
SRP Section: 03.09.02 - Dynamic Testing and Analysis of Systems Structures and Components
Application Section: 3.9.2

QUESTIONS for Engineering Mechanics Branch 2 (ESBWR/ABWR Projects) (EMB2)

Question 03.09.02-108:

The staff requested the applicant to provide the method for combining the uncertainties and bias errors and the effect of these on the resulting overall stress and vibration response prediction of the RPV internals in RAI 03.09.02-47c. The applicant responded by referencing CVAP sections 4.2.2.4 for the lower internals, 4.3.2.1 for the FDD, 4.5.1.1.4 for the upper internals, 4.6.3.2 for the CRGA and RCCA and section 4.7 for the heavy reflector tie rods. The staff did not find a discussion of the bias errors and uncertainties associated with the analysis of these components. The applicant is requested to discuss in quantitative and definitive terms, the methods for ascertaining and incorporating the bias errors and uncertainties in the calculation of the natural (resonant) frequencies, the peak response magnitude, mean FE response, the stress magnitude and tabulate the values of these bias errors and uncertainties.

Response to Question 03.09.02-108:

The modal analyses of the reactor pressure vessel internal (RPVI) components used the material properties established in the ASME Boiler and Pressure Vessel Code and the nominal (design) dimensions of the components. Therefore, no bias or uncertainties are incorporated into the analytical evaluations that determine the natural frequencies and mode shapes of the RPVI components. These design inputs are the most appropriate to consider in order to increase the likelihood of creating agreement of the frequency and mode shapes between the analytical predictions and hot functional test (HFT) results.

The response of a structure to random turbulence exhibits a Gaussian distribution. The analytical evaluation for random turbulence determines the root mean square (rms) response considering a standard deviation of "1σ". The 1-rms response in terms of displacement, stress and reaction force are determined for the RPVI components. The peak response to random turbulence for any structural location of the RPVI components is determined considering a standard deviation of "5σ" or the 5-rms response. A standard deviation of "5σ" results in a 5.734E-7 probability of excursion outside the 5-rms response value.

The acceptance criteria for random turbulence that is provided in Technical Report ANP-10306P incorporates these uncertainties via the methods discussed therein. Table 03.09.02-108-1 identifies the applicable section of ANP-10306P where the acceptance criterion for each of the RPVI components is defined. At locations where local structural discontinuities exist, fatigue strength reduction factors (FSRF) were applied to the 1-rms stress value before entry into the rms fatigue curves.

As stated above in this response, and in responses to Questions 03.09.02-71 and 03.09.02-112, no bias was introduced into the FE models or calculations; hence, the results appearing in ANP-10306P are essentially best-estimate values, without significant built-in conservatism. A general assessment of the accuracy of the finite element (FE) modeling approach is offered with the following write-up. In particular, an assessment of the uncertainty of the computed natural frequencies to within ± x percent of the actual frequencies and the computed amplitude, either integrated or modal, is within some factor or percent of the actual value provided. The analysis for the lower internal assembly was conducted for the HFT conditions, without the core, and that no credit was taken for reduced response due to the presence of the fuel assemblies (FAs).

The general assessment of the FE model accuracy is based upon the uncertainties associated with the follows attributes of the analysis.

- Firstly, uncertainties on structural compliance are estimated
- Secondly, uncertainties on fluid forcing function are derived
- Thirdly, combination of the above is made to determine the global uncertainty on the response levels

Uncertainty on Structural Compliance

The objective of the dynamic finite element model (FEM) is to predict the dynamic flexibility of the mechanical system. For a random vibrations analysis, this involves determining the frequency response functions (FRFs) between various degrees of freedom (DOFs). In order to be representative and correctly predict FRFs, the FEM must closely match the behavior of actual structures for all three types of forces:

- Restoring forces: linearity / discretization / boundary and interfaces conditions / material properties / manufacturing tolerances effects.
- Damping forces: structural, viscous, and flow-induced contributions.
- Inertia forces: structural, and hydro-dynamically induced.

Linearity: Restoring forces maintain proportionality to deflection as long as structural motion remains small enough so that neither material nor mechanical non-linearity is triggered. In the context of the RPVI response to FIV, the anticipated response is very small compared to the structural characteristic length (ratio ~10^{-5}). With respect to this condition, no significant uncertainty stemming from non-linear effects has to be accounted for. Therefore, the uncertainty associated with this aspect of the FEM is [ ] percent.

Formulation / Discretization: The restoring forces will be correctly predicted as long as the structural FEM adequately follows the real structure topology. The massive components (e.g., HR, LSP) are modeled with solid elements, the relatively thin components (e.g., CB) are modeled with plate or shell elements, and the relatively slender components (e.g., FAs) are modeled with beam elements. These rules have been strictly adhered to during FE model development. Therefore, the percent uncertainty is [ ] for this aspect of the FEM.

Similarly, the discretization effects are minimal. Considering the most limiting high-order modes, there is a minimum number of 10 elements per half-wavelength so that less than [ ] percent deviation on the structural frequency due to FE meshing effects could be realized. One exception to this is the HR "shell type" (N>1) modes, for which a coarse mesh was used (using only two elements through thickness, (refer to ANP-10306P, Figure 4-8, or Figure 03.09.02-108-1 below). In this case, a larger deviation can be anticipated, and was indeed found to be so when comparing to experimental results (deviation of [ ] percent and [ ] percent on frequencies for the two HR shell modes (N=2)) as shown in Technical Report ANP-10306P, Table 4-1. However, such a deviation could be ignored since a forcing function capable of exciting those shell modes is not anticipated. Therefore, the uncertainty associated with the effects of discretization in the FEM is accounted for as an uncertainty of a [ ] percent increase in the structural frequencies.

Boundary Conditions

The lower internals assembly rests on the CB flange of the RPV. The contact between these mating surfaces is maintained by lower internals assembly weight force, the weight of the FAs, and the preload created by the hold down spring (HDS), which together exceed the uplift forces due to hydraulic drag effects of the primary flow through the RPV internals (refer to the Response to Question 03.09.02-69 for additional information regarding the clamping load of these mating surfaces). Both the RPV and CB flanges are precisely machined so that little or no gap exists at this interface; and, therefore, the load path between those two components can be assured to be continuous around their circumference so that no reduction of apparent stiffness needs to be anticipated during normal operating conditions. The flange of the RPV itself is modeled as a rigid, immovable surface. This results in a slight overestimation of the overall stiffness of this mating surface; and, consequently, a minor increase in the natural frequencies of less than [ ] percent. The LSP and the radial keys are assumed not to come in contact during normal operating conditions and the results of the analysis verify this hypothesis. The RMS displacement value at this location has been determined to be below one third of the gap width. The probability that the vibration amplitude will exceed a 3σ value (or a 3rms response) is 2.7E-3 or less than 0.3 percent of the time. Therefore, the percent uncertainty is judged to be [ ] for this aspect of the FEM.

Interface Conditions (1 of 2):

Regarding the potential for contact between lower and upper internal assemblies, the interaction of these two components is not accounted for with the linear frequency domain type of analysis that is performed for the lower internal assembly. The width of the gap between these two components of [ ] is not very large compared to amplitudes of displacement that are anticipated at this location; and, therefore, the interaction of these two components remains largely unknown. The interaction of these two components, which could only be obtained through non-linear time domain solutions, is not performed to assess the degree of interaction.

The interaction of these two components would essentially add stiffness to the system, thereby increasing the frequency of the HR rocking mode and the CB beam mode. In order to evaluate the corresponding shift in frequency, a simple analysis has been conducted. First, the horizontal stiffness of the upper internal assembly has been evaluated through a detailed stress analysis using a FEM. A unit displacement is applied at the upper core plate (UCP) elevation to determine the stiffness of the upper internal assembly. This stiffness value is then used to extrapolate the updated modal frequency by estimating the additional strain energy stored into the upper internals. By assuming a small modal modification (i.e., no modification of the modal shape), the additional work strain energy is equal to:

$$\Delta E = \Phi_j^t \Delta K \Phi_j^t$$

Since the modification of the stiffness only occurs in one degree of freedom (i.e., the horizontal displacement of HR at its top elevation), this matrix equation degenerates to the scalar form:

$$\Delta E = U^2_{HRçTop} K_{UpperInternals}$$

Where, U is the horizontal component of displacement of the HR rocking mode at its top elevation. If the modes are normalized with respect to mass, the expression for work is numerically equal to squared modal pulsation:

$$\omega_j^2 = \frac{\Phi_j^t K \Phi_j^t}{\Phi_j^t M \Phi_j^t} = \Phi_j^t K \Phi_j^t \text{ since } \Phi_j^t M \Phi_j^t = 1$$

In the case of the HR rocking mode, the following numerical results are obtained:

- Horizontal stiffness of upper internal assembly:

  [ ] per Figure 03.09.02-108-2

- Modal displacement at HR top elevation (mass-normalized):

  [ ] per Figure 03.09.02-108-3

- Additional work due to the presence of the UCP interactions:

  ΔE = [ ]
  ΔE = [ ]

- Initial work in the absence of UCP interaction:

  E = [ ] per Figure 03.09.02-108-3

- Total work in the presence of UCP interaction:

  = [ ]

- New modal frequency:

[ ]

The maximum possible deviation in the frequency of the HR due to the contact between the lower and upper internals at the UCP elevation is equal to:

[ ] or approximately [ ] percent increase in the natural frequency.

Following the same approach for the case of the CB beam modes, the following results are obtained:

- Horizontal stiffness of upper internal assembly:

  [ ] per Figure 03.09.02-108-2

- Modal displacement of CB at the elevation equivalent to the top of the HR (mass normalized):

  [ ] per Figure 03.09.02-108-4

- Additional work due to the presence of UCP interaction:

  [ ]
  [ ]

- Initial work in the absence of UCP interaction:

  [ ]

- Total work in the presence of UCP interaction:

  [= 2577 + 392 = 2969 mJ (26.1 lbf-in)]

- New modal frequency:

[ ]

The maximum possible deviation in the frequency of the CB due to the contact between the lower and upper internals at the UCP elevation is equal to:

[ ] or approximately [ ] percent increase in the natural frequency.

Interface Conditions (2/2):

A large number of interfaces exist between the 12 individual slabs that comprise the HR component. The slabs are held tightly together with [ ] tie rods; hence, no separation can occur. However, this does not guarantee that there is perfect continuity of displacements at interfaces between the slabs, even though the compression of these mating surfaces is tightly controlled. Consequently, the stiffness of the HR might be overestimated. However, this has no influence whatsoever on the dynamic response of the lower internals, since the HR essentially behaves as a rigid body. This can be demonstrated by examining the distribution of modal strain energies, provided in Figure 03.09.02-108-5. As explained in t ANP-10306P, Section 4.2.3.2 and Figure 4-15, the modes that significantly contribute to the FIV response of the lower internals are the HR beam modes (Rank 3 and 4) and more importantly the CB beam modes (Rank 11 and 12). For these modes, the fraction of strain energy stored into the HR is [ ] percent (for HR rocking mode) and only [ ] percent (for CB beam modes), as can be seen in Table 03.09.02-108-2.

Consequently, even a large distortion on the HR flexibility would only marginally affect the results. For example, reducing the HR stiffness by a factor of two would diminish the corresponding total strain energy of Modes 3 and 4 by [ ] and reduce the HR rocking modes frequency by about [ ] percent. The same reasoning applied to the CB beam mode shows that the modal frequency would be reduced by [ ] percent.

Manufacturing Tolerances:

As can be seen in Table 03.09.02-108-2, the CB has the most significant influence to the overall stiffness of the lower internal assembly and for the frequency of the significant modes. Consequently, the tolerance on CB shell thickness is the major contributor to the uncertainty of its stiffness. FEM calculations have been conducted using the nominal thickness value considering a [ ] percent value of tolerance on its thickness, conservatively assuming an overall stiffness controlled by local bending at CB flange connection. The results of this calculations show [ ] percent uncertainty on overall stiffness.

Material properties:

Uncertainty on elastic properties (Young Modulus) of material are small, and can be considered to be less than [ ] percent.

Damping forces

As summarized in ANP-10306P, Table 4-7, the damping ratios of [ ] percent and [ ]percent have been respectively used for HR rocking mode and CB beam modes, corresponding to HFT conditions. These values represent the sum of two major contributors:

- Structural damping [ ] and viscous damping [ ] for HR rocking modes.
- Structural damping [ ] and flow-induced damping [ ] for CB beam modes.

Uncertainties on structural damping are significant. A value of [ ] percent has been selected, but large deviation could be expected, so that credible values range from [ ] percent to [ ] percent.

Uncertainties associated with the magnitude of the viscous damping are not important since the formula used in ANP-10306P, Section 4.2.5.3.3, have been benchmarked by AREVA NP and were found to provide consistent estimation of the damping to within a relative uncertainty of [ ] percent or better; so the actual values could range between [ ] percent to [ ] percent. Therefore, a credible range for the HR rocking modal damping ratio would be [ ] percent; or, equivalently, a [ ] percent relative uncertainty.

Uncertainties associated with the magnitude of the damping for the CB beam modes created by the flow are limited since the contribution has been extracted from the mockup. Secondly, because the hydro-elastic similitude was achieved, the only correction applied was through the consideration of the density for water between mockup and prototype conditions (see ANP-10306P Section 4.2.5.3.2). Therefore, the uncertainty associated with this damping mechanism is insignificant. Consequently, a credible range for the damping ratio for the CB beam mode would be [ ] percent to [ ] percent; or, equivalently, [ ] percent relative uncertainty.

Note that in case of normal operation, with the core loaded in the RPV, these values would be increased by the presence of the fuel assemblies. Past experiences shows that for the CB beam mode, damping ratio of no less than [ ] percent are observed with the typical range being between [ ] percent damping.

Inertia forces

The inertia forces are linked to the distribution of mass within the structure, which is generally well known; therefore, a minimal uncertainty (± [ ] percent) is assumed. However, in the case of the lower internals, most of the inertia is controlled by hydrodynamic forces. This is illustrated in Figure 03.09.02-108-6. As can be seen with this figure for all modes except the CB beam mode, the hydro-dynamically induced terms represent over 98 percent of total kinetic energy.

As known from two-dimensional analysis of flat plates (e.g., ASME Section III, Appendix N-1450), as soon as ratio of the outer radius and inner radius is close to unity, the hydrodynamic mass terms become inversely proportional to thickness of the fluid gap. In the case of modes 1 to 10, the HR/CB annulus has the most significant influence for the modal mass. Therefore, the uncertainties associated with the hydrodynamic mass are directly linked to the manufacturing tolerances of the HR/CB water annulus. Assuming an [ ] percent uncertainty for the thickness of this water annulus [ ] creates an [ ]percent uncertainty with the modal mass; and, therefore, a [ ] percent uncertainty with all modal frequencies (for modes with rank 1 to 10).

For CB beam modes (rank 11 and 12), the hydrodynamic mass represents approximately [ ] of the total energy. Furthermore, the uncertainty with the thickness of the downcomer is much lower (less than [ ] percent). Therefore, a global [ ] percent of uncertainty for the modal mass will be conservatively assumed, which implies a [ ] percent uncertainty with the modal frequencies.

Uncertainty with the Forcing Function for Turbulence

The uncertainties on the forcing function encompass the following contributors:

- Uncertainties on measurements.
- Uncertainties on parameters identification.
- Uncertainties on reactor flow rates.

Uncertainties with the measurements for dynamic pressure: As indicated in Response to Question 03.09.02-114, an overall (i.e. broadband) accuracy of [ ] percent or better was achieved during experimental tests. It is noted that since the averaged values have been used for more than 10 sensors, the actual value is probably much lower, so that this is more a bounding value than a typical value.

Uncertainties with the identification of parameters: The spectral parameters (e.g., slopes and corner frequencies) are averaged quantities performed in the frequency domain that are obtained from the best-fit of the raw data curves. These parameters are relatively immune to dispersions and pollutions of the spectra so a [ ] percent uncertainty with these values is appropriate. Similarly, the correlations lengths and angles are averaged quantities in the space domain so these parameters are also immune to measurement noise. A [ ] percent uncertainty in the value of these terms will be used.

Uncertainties with the flow rates: Flow rates in the test setup are measured with high-quality electromagnetic flow meters. The uncertainty in the flow rate is about [ ] percent. However, the uncertainty with the flow rates for the full-scale design during reactor operation is equal to [ ] percent. This value is based upon the difference between the design mechanical flow rate and best estimate flow rate.

The uncertainty in the velocity of the fluid in the downcomer created by the manufacturing tolerance in the width of the downcomer [ ] inches and the concentricity between the RPV ID and the CB OD [ ] inches is [ ] as shown with the following calculations. The concentricity of 0.1 inches between the RPV ID and the CB OD will not change the overall flow resistance in the downcomer region and therefore the increase in the fluid velocity from this manufacturing tolerance is negligible. However, this uncertainty is considered to be accounted for by the increase in the fluid velocity that is determined below when based upon the reduced flow area created by the tolerance in the width of the downcomer and applied to the full circumference and length of the downcomer annulus.

Since these sources of uncertainties are statistically independent, they are combined quadratically. The combined effect of these uncertainties in the flow rate or the fluid velocity in the downcomer is equal to approximately [ ]. This uncertainty with the flow velocity results into a [ ] uncertainty with the RMS fluid induced force and an [ ] percent uncertainty on the spectral content of the pressure PSD for turbulence.

Uncertainty with the Level of Response

The level of response is obtained through integration of the fluid forcing function effects on the entire CB surface; hence, a double integration with respect to space and a single integration with respect to frequency. As stated in ANP-10306P, Section 4.3.2.1, the process used in the ANSYS calculation makes no further simplification, and employs a close-form integration technique for the frequency-wise integration, as well as the full modal basis, so that no significant bias or uncertainty is further introduced by the calculation scheme. An uncertainty of [ ] is assessed for this consideration. Therefore, the uncertainty on response levels is entirely controlled by uncertainties on the structural compliance and on the fluid forcing function, as discussed in the previous paragraphs.

In order to quantify the overall uncertainties, it is not practical to use the numerical scheme presented above and used in the development of ANP-10306P. Instead, simple formulas will be considered to capture the essential features of the structural response.

The mean-squared response for any DOF on the structure can be theoretically determined from the following expression:

$$S_{di}(\omega) = \sum_{j=1}^{n}\sum_{k=1}^{n}\Phi_{ij}\Phi_{ik}\left(\sum_{l=1}^{n}\sum_{m=1}^{n}H_j^*(\omega)H_k(\omega)S_{lm}(\omega)\right)$$

Where:

S_{di} denotes the i[th] DOF displacement response PSD

Φ_{ij} and Φ_{ik} respectively denote the modal displacement at the i[th] DOF for j[th] and k[th] eigenvectors

$H_j(\omega)$ (resp. $H_k(\omega)$) respectively denote the modal displacement frequency response function for the j[th] (resp. k[th]) mode (complex quantity)

$S_{lm}(\omega)$ denotes the nodal force cross PSD between DOFs *l* and *m* (complex quantity).

This complicated equation can be reduced to a much simpler form provided that:

1. one mode governs the overall response of the structure
2. the auto power spectra are independent of space and the cross power spectra depend on the distance between points (or nodes) and not on the location of the points (or nodes) on the structure. This is to say that the PSD for turbulence is homogenous through out the surface of the structure (space wise) and the coherence function depends only upon the distance of separation between two points on the structure.
3. the spectrum for the forcing function is a slowly varying function (smooth) and the cutoff frequency is lower that the first modal frequency

For these circumstances, the double summation with the modal content can be removed, and only the direct modal terms are needed. Further, the value for the nodal force PSD can be taken out of the innermost double summation (over space) and lastly, the variance of the response becomes equal to the sum of a quasi-static part, and a resonant part. The equation above can now be simplified to the following expression (retaining only one mode of order *n*):

$$< S_{di}{}^2 > \approx \Phi_{ni}^2\left(\frac{< F^2 >}{m_n^2\omega_n^4} + \frac{PPSD(\omega)I_{nn}(\omega)}{8m_n^2\varepsilon_n\omega_n^3}\right)$$

Where:

<F²> denotes the variance of the net total force applied on the structure

m_n = modal mass (generally equal to unity)

ω_n = resonant pulsation

ε_n = modal damping ratio (fraction of critical)

PPSD = Pressure Power Spectral Density

I_{nn} = joint acceptance integral of mode n $I_{nn}(\omega) = \int_{surface} \Phi_n(x_1)\Phi_n(x_2)\Gamma(x_1,x_2,\omega)dx_1dx_2$

In the previous equation, the first term represents the quasi-static structural response to the fluid forcing function, while the second term corresponds to the so-called Miles formula. For example, in the case of the displacement response of the LSP along reactor zero degree axis (see ANP-10306P, Figure 4-16), it can be seen that both terms contribute approximately [ ] of total response. Using this form of the equation, it is possible to combine the previous uncertainties obtained for the individual parameters to assess the overall uncertainty.

Uncertainty with the quasi-static term:

Like any static response, the overall uncertainty is the combination of the uncertainty on overall force and stiffness. From the previous discussion, the total uncertainty on stiffness is;

$\beta_{stiffness}=$

$$\sqrt{\beta^2_{FEMdiscretization.} + \beta^2_{BoundaryConditions} + \beta^2_{InterfaceConditions} + \beta^2_{ManufacturingTolerances.} + \beta^2_{MatProperties}}$$

All these terms have been estimated in the paragraphs related to structural compliance. A factor of two is applied to convert uncertainties associated with frequencies to uncertainties associated with stiffness. Inconsideration of the response of the CB beam mode, this will yield;

$\beta_{stiffness} =$ [ ]

Regarding the [ ] percent uncertainty associated with the quasi-static results, it is noted that this value is larger than the [ ] percent offset value that was obtained with the HYDRAVIB mockup flow test. There are two reasons for this. First, the primary contributor of the [ ] percent uncertainty is due to the interaction between lower and upper internals at the UCP elevation which was non-existent in the HYDRAVIB test. Secondly, the uncertainty assessed for the deviations due to manufacturing tolerances have been assumed to be uniform for the entire CB shell surface, which is highly unlikely.

A bounding value for the uncertainty of the CB stiffness (on the negative side) can be estimated by removing the uncertainty due to contact with upper internals (i.e. the β_{IC} term). Similarly, the artificial stiffening effect due to rigid boundary condition or FEM discretization can also be removed. Therefore, the two different values of uncertainty are obtained as follows;

$$\beta_{stiffness} = \sqrt{\beta^2_{FEMdiscretization.} + \beta^2_{BoundaryConditions} + \beta^2_{ManufacturingTolerances.} + \beta^2_{MatProperties}}$$

$$\beta_{stiffness} = [\quad\quad]$$

$$\beta_{stiffness} = \sqrt{\beta^2_{InterfaceConditions} + \beta^2_{ManufacturingTolerances.} + \beta^2_{MatProperties}}$$

$$\beta_{stiffness} = [\quad\quad]$$

The uncertainty with the variance of the forcing function is the combination of two independent contributors, therefore:

$$\beta_{forcing\_function} = \sqrt{\beta^2_{Measurements.} + \beta^2_{FlowRates}}$$

$$\beta_{forcing\_function} = [\quad\quad]$$

Therefore, the total uncertainty on variance of quasi-static contribution is equal to:

$$\beta_{quasi\_static\_response} = \sqrt{\beta^2_{stiffness} + \beta^2_{forcing\_function}}$$

$$\beta_{quasi\_static\_response} = [\quad\quad]$$

$$\beta_{quasi\_static\_response} = [\quad\quad]$$

It is noted that the overall uncertainty for the increased response is largely controlled by uncertainty of the flow rate.

Uncertainty with the resonant term:

In addition to the uncertainties accounted for in the static response, the following contributions must be evaluated:

- Uncertainty regarding resonant frequency
- Uncertainty regarding Pressure PSD amplitude at resonant frequency
- Uncertainty regarding Joint Acceptance Integral value at resonant frequency
- Uncertainty regarding damping ratios

The uncertainty regarding resonant frequency is:

$$\beta_{frequency} = \sqrt{\beta^2_{stiffness\_terms} + \beta^2_{mass\_terms}}$$

In the case of CB beam-type response, this will yield an uncertainty of;

$\beta_{frequency}=$ [redacted]

$\beta_{frequency}=$ [redacted]

From Technical Report ANP-10306P, Section 4.2.2.4.1, the amplitude of the pressure PSD at the resonant frequency is:

[redacted]

The consideration of the B_2 index stems from the fact that all structural resonant frequencies are above the cutoff frequency. This can be rearranged by lumping the constant terms into a single value as follows

[redacted]

Therefore, the total uncertainty on PSD amplitude at resonant frequency reads

$$\beta_{PSD\_at\_resonance} = \sqrt{((3+B_2)\beta_{velocity})^2 + (B_2\beta_{frequency})^2}$$

For the response of the CB beam mode type, the uncertainty is:

$\beta_{PSD\_at\_resonance} =$ [redacted]

$\beta_{PSD\_at\_resonance} =$ [redacted]

Estimation of the uncertainty associated with the evaluation of joint acceptance integral (JAI) at the resonant frequency requires usage of an approximate closed form solution. It is a common practice to use a separable form for the evaluation of the JAI on a cylindrical shell. The JAI for a two-dimensional surface is simply equal to the product of the one dimensional JAI along each of the two axis. In the case of the CB shell, this can be defined as follows:

$$JAI_{CB}(\lambda_{axial}, \lambda_{circumferential}) \approx JAI_{beam}(\lambda_{axial}) JAI_{shell}(\lambda_{circumferential})$$

For the case where both the axial and circumferential correlation lengths are small in comparison to the structural dimensions and the bending wavelength, further simplifications can be made to the definition of the JAI:

$$JAI_{beam}(\lambda_{axial}) \approx \frac{2\lambda_{axial}}{L}$$ where, L is the length of the shell

$$JAI_{shell}(\lambda_{circumferential}) \approx \frac{2\lambda_{circumferential}}{2\pi R}$$ where, R is the radius of the shell

Both of these correlation lengths have linear dependency with respect to the f/V ratio; hence, it follows that JAI can be written as:

$$JAI_{CB}(\lambda_{axial}, \lambda_{circumferential}) \approx C_{axial} C_{circumferential} \left(\frac{V}{f}\right)^2$$

Finally, the total uncertainty on JAI at resonant frequency reads:

$$\beta_{JAI\_at\_resonance} =$$

$$\sqrt{\beta^2_{axial\_correlation\_length} + \beta^2_{circumferential\_correlation\_length} + (2\beta_{frequency})^2 + (2\beta_{FlowRate})^2}$$

Numerically, this will yield:

$\beta_{JAI\_at\_resonance}$= [ ]

$\beta_{JAI\_at\_resonance}$= [ ]

The amplified response term is:

$$< S_{di}^2 >= C \frac{PPSD(\omega) I_{nn}(\omega)}{\varepsilon_n \omega_n^3}$$

The uncertainty on the variance of the amplified response is;

$$\beta_{amplified\_response} = \sqrt{(\beta_{PPSD} + \beta_{JAI} + 3 \times (\beta_{resonance\_frequency}))^2 + \beta^2_{damping}}$$

Since the first three terms are mutually partially correlated, they are conservatively added algebraically, while the last term, being independent of the rest of the summation, is added quadratically. Numerically, this yields:

$\beta_{amplified\_response}$= [ ]

$\beta_{amplified\_response}$= [ ]

Uncertainty with the global RMS LSP motion:

In the case of the response of the LSP, the uncertainty on the RMS level is simply estimated based upon the total variance being equal to the sum of the variance of the quasi static term and the amplified term. Both terms account for approximately half of the total variance, as seen with Figure 03.09.02-108-7 and also depicted in ANP-10306P, Figure 4-23 and Figure 4-24. In this case, the total uncertainty is equal to average of individual uncertainties as written below;

$$\beta_{total\_response\_variance} \approx 0.5 \times \beta_{quasi\_static\_response} + 0.5 \times \beta_{amplified\_response}$$

Numerically, this yields:

$$\beta_{total\_response\_variance} = \left[\qquad \right]$$

$$\beta_{total\_response\_variance} = \left[\qquad \right]$$

Note that with the expression for "F_{lower}", the square root of the reciprocal of the total response variance term is used to determine the lower bound response and differs from the method by which the upper bound value is computed. The reason for this difference is due to the mathematical manner by which the bias and uncertainty terms have been computed to assess the lower bound response. Since the lower bound variance terms have been computed with a positive variance, as opposed to a negative variance, it is mathematically more appropriate to determine the lower bound response in the manner that is performed above to obtain the lower bound response.

The factors to be applied on the best estimate RMS levels to obtain upper and lower bounds are:

$$F_{upper} = \left[\qquad \right]$$

$$F_{lower} = \left[\qquad \right]$$

Or, equivalently, the following percentages [+19%, -24%].

From ANP-10306P, Table 4.9, the best estimate value for the displacement of the LSP for the full-scale design during HFT is of [ ] RMS. Considering these uncertainties, the following interval of displacement is obtained:

$$\left[\qquad \right]$$

These values are consistent with the results obtained with the HYDRAVIB mockup testing. An offset of [ ] percent on RMS levels had been obtained between the numerical and experimental results but, again some uncertainties where non existent during this benchmark. Most importantly, the uncertainty with the flow rate did not exist since it was precisely known during the HYDRAVIB flow tests. A general conclusion is that the uncertainty introduced by numerical simulation is lower than that related to knowledge of actual conditions during operations.

Uncertainty with the global RMS HR motion:

Applying the same process to assess the uncertainty for the response level of the HR at its upper elevation (the label HR_{A2} in Figure 03.09.02-108-7) yields a supplementary term which accounts for approximately [ ] percent of total response variance.

$$\beta_{total\_response\_variance} \approx 0.5\beta_{quasi\_static\_response} + 0.05 \times \beta_{amplified\_response\_HR} + 0.45 \times \beta_{amplified\_response\_CB}$$

Only the term related to amplified response of HR must be evaluated.

Compared to the previous analysis, the uncertainties on the HR dominant frequency are higher due to:

- possible increase of stiffness due to interface conditions between the upper and lower internals, implying an increase in frequency of about [ ] (see Interface Conditions (1/2) section of this response)
- possible reduction of stiffness due individual HR slabs, implying a decrease in frequency of about [ ] percent (see Interface Conditions (2/2) section of this response)
- uncertainty on mass, implying an uncertainty on frequency of about [ ] (see Inertia Forces section of this response)

Therefore, the combined uncertainty on frequency is:

$\beta_{frequency} = \sqrt{(0.05^2 + 0.055^2}$ =7.4% (decrease)

$\beta_{frequency} = \sqrt{(0.08^2 + 0.055^2}$ =9.7% (increase)

For convenience, an envelope value of 10% will be applied.

The uncertainty relative to PSD at resonance can be estimated as previously

$$\beta_{PSD\_at\_resonance} = \sqrt{((3 + B_2)\beta_{velocity})^2 + (B_2\beta_{frequency})^2}$$

$\beta_{PSD\_at\_resonance} = \sqrt{((3 + 2.60) \times 0.082)^2 + (2.60 \times .10)^2}$ =0.53 (increase and decrease)

The uncertainty relative to JAI is also obtained:

$\beta_{JAI\_at\_resonance}=$

$$\sqrt{\beta^2_{axial\_correlation\_length}+\beta^2_{circumferential\_correlation\_length}+(2\beta_{frequency})^2+(2\beta_{FlowRate})^2}$$

$\beta_{JAI\_at\_resonance}=$ [ ]

The uncertainty on damping has been evaluated to be equal to [ ] percent. The total uncertainty on variance due to HR amplified response is:

$$\beta_{amplified\_response}=\sqrt{(\beta_{PPSD}+\beta_{JAI}+3\times(\beta_{resonance\_frequency}))^2+\beta^2_{damping}}$$

$\beta_{amplified\_response}=$ [ ]

There is an uncertainty of about a factor of [ ] for the contribution of HR amplified response. However, this term only represents [ ] percent of the total response variance, hence doubling its contribution would mean only adding [ ] percent of the total response variance, or equivalently, adding [ ] percent to the RMS level. Even in that extreme case, contribution for the HR rocking motion is of secondary importance and uncertainties are almost unchanged compared to that of obtained at the LSP. So the [ ] percent interval of uncertainty is used here. Numerically, this means that starting from the best estimate value of [ ] RMS for the displacement of the HR, as indicated in ANP-10306P, Table 4.9, the following interval of displacement is obtained:

[ ]

Section 4.2.7.3 will be added to ANP-10306P to provide an overview and a summary of the degree of uncertainty in the analysis for the FIV results.

FSAR Impact:

The U.S. EPR FSAR will not be changed as a result of this question.

Technical Report Impact:

ANP-10306P, "Comprehensive Vibration Assessment Program for U.S. EPR Reactor Internals Technical Report," Revision 1, will be revised as described in the response and the indicated on the enclosed markup.

Table 03.09.02-108-1: Acceptance Criteria for Random Turbulence for the RV Internal Components

U.S. EPR RV Internals Component	Section of ANP-10306P
RV Lower Internal Assembly	Section 4.2.6
Flow Distribution Device	Section 4.3.3
RV Upper Internals (control rod guide assembly (CRGA) column supports, normal column supports, level measurement probe column supports, and guide tubes)	Section 4.5.2
CRGAs and rod cluster control assemblies (RCCA)	Section 4.6.4

Table 03.09.02-108-2: Distribution of Modal Strain and Kinetic Energy

[
]

Figure 03.09.02-108-1: FEM of Lower Internal Assembly

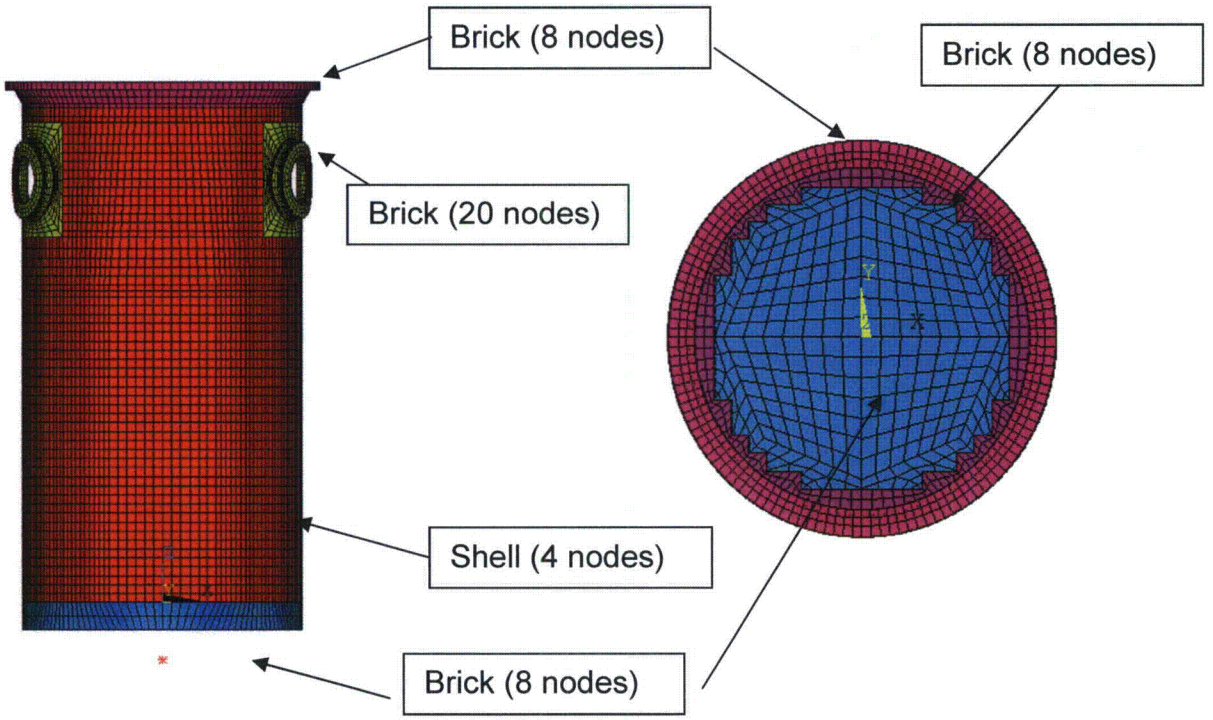

Figure 03.09.02-108-2: Estimation of Upper Internals Horizontal Stiffness (1/4 Scale Model)

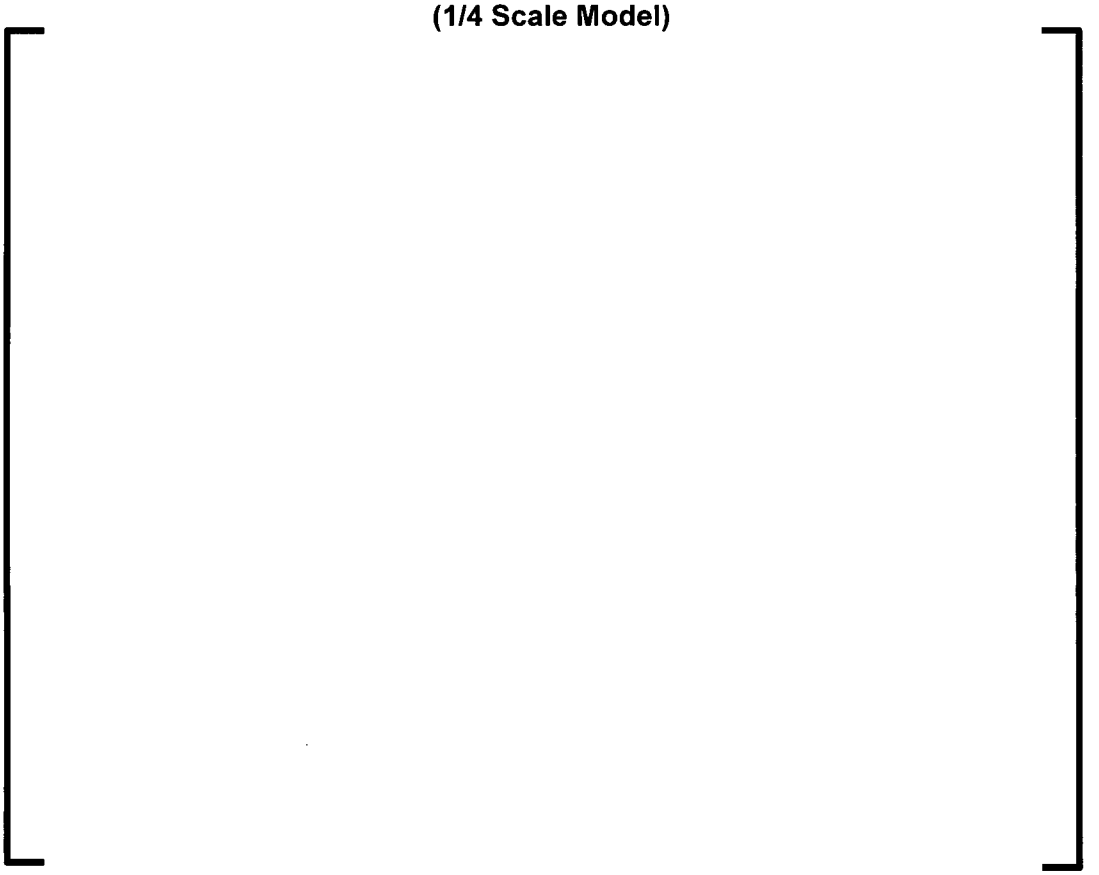

Figure 03.09.02-108-3: Heavy Reflector Rocking Mode

(mass normalized amplitude)

Figure 03.09.02-108-4: Core Barrel Beam (Mass normalized amplitude)

Figure 03.09.02-108-5: Strain Modal Energy Ratios

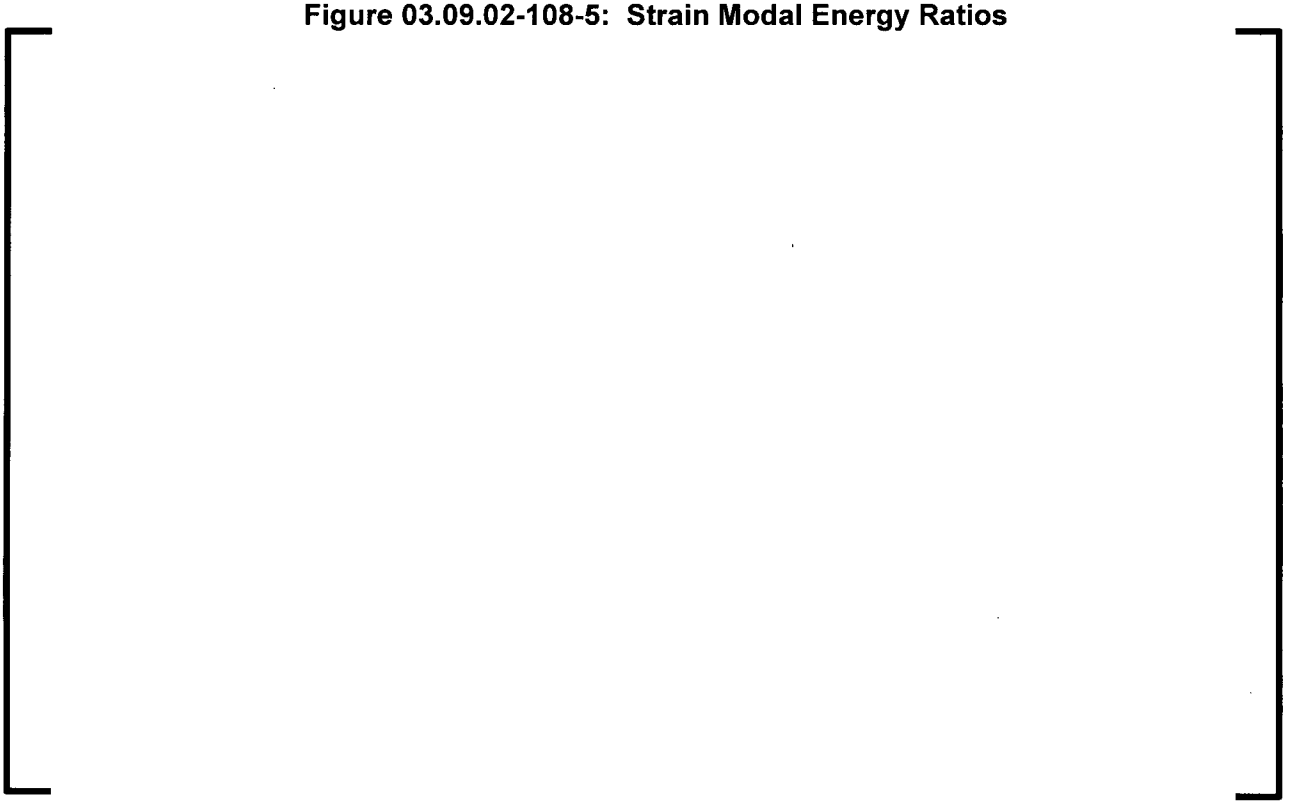

Figure 03.09.02-108-6: Kinetic Modal Energy Ratios

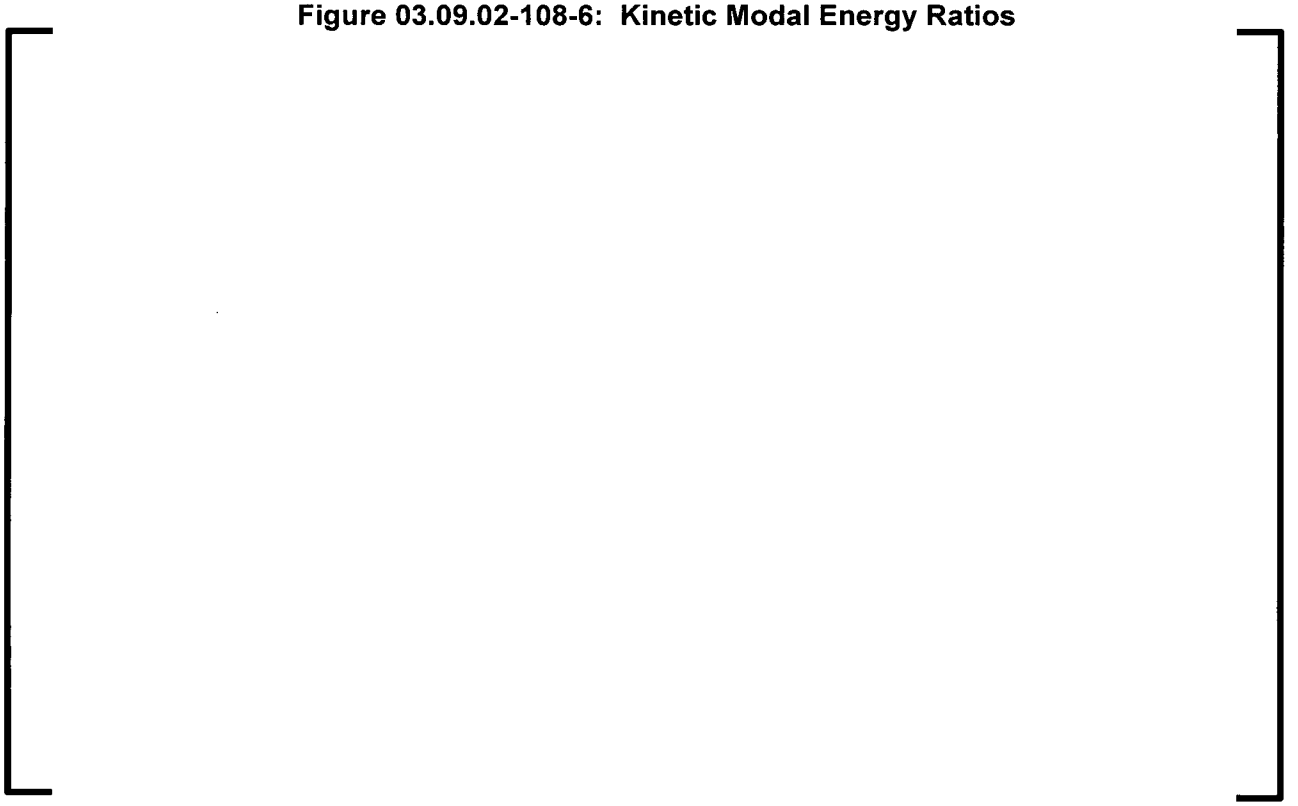

Figure 03.09.02-108-7: Energy Distribution of Horizontal Component of Motion

ANP-10306NP Technical Report Markups

4.2.7.2 Stress Levels

The distribution of stress is displayed in Figure 4-26. As expected, peak stresses are located at the junction between the CB shell and the flange (local bending occurs in this region) with secondary stress concentrations in the vicinity of the nozzles.

A maximum stress of [ ] MPa, rms (or [ ] psi, rms) is shown in Figure 4-26 at the CB flange elevation. ~~Considering~~Applying a fatigue strength reduction factor (FSRF) of [ ] for the cylinder to flange juncture, a weld quality factor (f=1) for dynamic loading dynamic as prescribed by ASME Section III, Table NG-3352-1 for the category C, Type I weld joint, and the scaling factor of [ ], a peak stress of approximately [ ] psi, rms is obtained for the full power normal operating condition.

To evaluate the RV lower internals for fatigue, the number of cycles per unit time is taken from the displacement results (See Table 4-10). Considering a crossing frequency of [ ] Hz and based upon 60 years of continuous operation (i.e., assuming a 100 percent capacity factor), this yields a number of cycles of about [ ] . Using ~~Table 4-21~~Figure 4-21 and fatigue "C", the allowable number of cycles for the [ ] psi, rms peak stress is > 10^{13} cycles. Therefore the fatigue usage factor is less than [ ] The endurance limit of approximately [ ] psi, rms at [ ] cycles is greater than four times the stress in the CB ([ ] psi, rms). ~~an endurance limit of approximately 6000 psi, rms is estimated, which is well above the stress in the CB, which is 850 psi, rms.~~ Therefore, high cycle fatigue failure resulting from the random turbulence in the RV downcomer is not predicted to occur.

4.2.7.3 Uncertainty and Bias in the Predicted Response

The structural model for the lower internal assembly evaluated the nominal (design) dimensions of the components to determine the natural frequencies and mode shapes of these components. As such, the analytical model does not specifically consider the manufactured tolerances associated with the geometry of the structures and the differences in material properties values established in the ASME code and the as-built values. Since the analytical results will be compared to HFT results, the appropriate practice is to consider the "best estimate" design inputs in order to obtain the best agreement between the analytical and field test results. The implication of this approach is addressed in the following paragraph.

The fluid-structure coupling mechanism for random turbulence is weak in that the flow field induced by the structural motion is linearly superimposed on the incident flow field. In contrast, a strongly coupled fluid-structural system, which is characterized by large structural motion, will induce fluid velocities and completely distort the incident flow field. Vortex-shedding induced vibration and fluid-elastic instability of heat exchange tubes are examples of strongly coupled fluid-structure systems. With these strongly fluid-structural coupled systems, the sensitivity of the FIV mechanism to the natural frequencies of the components becomes fundamental as to whether or not this mechanism is active and the strength of the response. For the weakly fluid-

RAI 422
Q. 03.09.02-108

structure coupling associated with random turbulence, the relationship between the natural frequencies and the response of the structure is not as strongly associated; therefore, the slight variation in the natural frequencies that would be attributed to manufactured tolerances and material property variations will not significantly alter the forcing function and the response of the structure.

Nonetheless, a general assessment of the FE model accuracy based upon the uncertainties associated with various attributes of the analysis was undertaken to establish an overall range of uncertainty in the computed frequencies and the level of response. An overall summary of the range of uncertainties in the modal frequencies and response level of the RPVI is provided below. The assessment of the uncertainties associated with the analyses can be itemized into the following three categories:

- Uncertainties on structural compliance.
- Uncertainties on fluid forcing function.
- Combination of the above to assess the global uncertainty on the response levels.

Uncertainty on Structural Compliance

The uncertainty associated with the dynamic flexibility of the RPV lower internal assembly was assessed for:

- Restoring forces: linearity, discretization, boundary and interfaces conditions, material properties, manufacturing tolerances effects.
- Damping forces: structural, viscous, and flow induced contributions.
- Inertia forces: structural, and hydro-dynamically induced.

Uncertainty with the Forcing Function for Turbulence

The uncertainties on the forcing function for turbulence considered the following contributors:

- Uncertainties with the measurement of dynamic pressures.
- Uncertainties with the spectral parameters (slopes and frequencies).
- Uncertainties on reactor flow rates.

Uncertainty with the Fundamental Frequency of the CB

As stated in Section 4.2.8, the response of the lower internals to random turbulence is primarily dominated by the fundamental beam mode of the CB. From Table 4-5, the best estimate value for the fundamental frequency of the CB beam modes are [ ] Hz. Considering the uncertainties itemized above, the percent uncertainty with the CB beam mode frequencies are [ ] percent to [ ] percent to obtain the following range of frequency:

- [ ]

RAI 422
Q. 03.09.02-108

Uncertainty with the Level of Response of the CB at the LSP Elevation

From Table 4-9, the best estimate value for the displacement of the LSP for the full scale design during HFT is [ ] mil, rms. Considering the uncertainties itemized above, the percent uncertainty for the turbulent response of the CB beam mode is [ ] percent to [ ] percent to obtain the following interval of displacement:

- [ ]

This value is consistent with the results obtained with the HYDRAVIB mockup testing. An offset of [ ] percent on rms levels was obtained between the numerical and experimental results.

Uncertainty with the Frequency of the HR Beam Mode

From Table 4-5, the best estimate value for the fundamental frequency of the HR beam mode (modes 3 and 4 or the "rocking modes") is [ ] Hz. Considering the uncertainties itemized above, the percent uncertainty with the HR beam mode frequency is [ ] percent to obtain the following range of frequency:

- [ ]

Uncertainty with the Level of Response of the HR at Location / Elevation "HR_A1"

From Table 4-9, the best estimate value for the displacement of the HR at the elevation or location "HR_A1" for the full scale design during HFT is [ ] mil, rms. Considering the uncertainties itemized above, the percent uncertainty for the turbulent response of the HR beam mode is [ ]. Even in that extreme case, the contribution for the HR rocking motion is of secondary importance and uncertainties are almost unchanged compared to that of obtained at the LSP. So the [ ] percent interval of uncertainty obtained for the response of the CB at the LSP elevation is used here to obtain the following interval of displacement for the HR:

- [ ]

Uncertainty with the Stress Levels in the CB

The uncertainly in the computations for stress in the CB are directly proportional to uncertainties reported above for its dynamic response. Additionally, a FSRF of 3.0 is considered in the stress results reported in Section 4.2.7.2 to account for the peak stress effects created by the structural discontinuity of the CB cylinder and the CB flange. From Section 4.2.7.2, a peak stress of 850 psi, rms is reported. Considering the range of uncertainties reported above for the response of the CB, the following range of stress at the CB flange elevation was obtained:

- [ ]

This maximum stress is just less than four times the endurance limit of 4000 psi, rms at 10^{10} cycles reported in Section 4.2.7.2. Therefore, high cycle fatigue failure is not predicted to occur.

RAI 422
Q. 03.09.02-108